16TH EUROPEAN CONFERENCE ON
EARTHQUAKE ENGINEERING THESSALONIKI
18 - 21 JUNE 2018

NUMERICAL STUDIES ON MULTI-CELL CFT COLUMNS WITH DOUBLE-LAYER CIRCULAR STEEL TUBES

Wencong LI[1]

ABSTRACT

Nowadays, height, scale and shape of super-tall buildings and structures with height over 300 meters have been successively renewed in the world. In order to meet the demands of the age and architectural design, mega-columns with excellent seismic and wind-resistance performance are required to improve global stability of them. In this study, multi-cell CFT columns with double-layer circular steel tubes, which are developed from the concrete-filled double-layer circular steel tubular column through installing the separating steel plates and longitudinal stiffeners, are proposed for the mega-column. Numerical studies on simple multi-cell CFT columns without the longitudinal stiffeners are carried out using OpenSees to investigate the contributions of the separating steel plates to the seismic performance of the multi-cell CFT column.

Keywords: Mega-Column; Multi-Cell CFT column; Double-Layer steel tubes; Separating steel plate; Numerical study

1. INTRODUCTION

1.1 Demand for Mega-Column

Nowadays, height, scale and shape of super-tall buildings and structures with height over 300 meters have been successively renewed in the world. In order to meet the demands of the age and architectural design, mega-columns with excellent seismic and wind-resistance performance are required to improve global stability of them. Generally, the mega-columns are expected to be located at the building perimeter, therefore they can more effectively balance the overturning moment of the building caused by the lateral forces such as wind and seismic loads. The mega-columns in the perimeter of the super-tall building, which need to support the dead load in proportion to the height of the building and the additional axial load generated by the overturning moment, are key structural members, and they are also expected to have excellent seismic performance under high axial load.
On the other hand, for mega-columns used in the actual projects such as (Ding et al. 2011, Liu et al. 2012 and Liu et al. 2012), the details of cross sections are very complicated, and the constructions are too hard.

1.2 CFT Column

Concrete filled steel tube (abbreviated as CFT hereinafter), which is a kind of composite structural member consisting of a steel tube infilled with concrete, has a number of distinct advantages over an equivalent steel, reinforced concrete, or steel-reinforced concrete member, because combined effects of the steel and concrete in the cross section optimize the strength and stiffness of the section. Therefore, the CFT structure has been noticed as the fourth structure which follows steel structure, reinforced concrete structure and steel reinforced concrete structure in all over the world. For utilization and extension of the CFT, a series of Japan-US Cooperative Earthquake Research Program since 1995 (Mukai et al. 1995-1998) and other many researches such as (Kawano et al. 1996, Fujimoto

[1]Associate Professor, Toyo University, Kawagoe, Japan, f995095@hotmail.com

et al. 1997, Tsuda and Matsui 1998, Yamamoto et al. 2002, Gould and Harmon 2002, Saisho et al. 2003, and Georgios and Dennis 2004) have been conducted.
In structural design of high-rise buildings in Japan, the key columns are often selected as CFT columns.

1.3 CFDLT Column

Recently, a relatively simple cross-section of column with concrete-filled double-layer steel tubes shown in Figure 1 was proposed by Li (2017a) to decrease the axial compressive strain; and quasi-static cyclic test of the proposed concrete-filled double-layer steel tubular column (abbreviated as CFDLT column hereinafter) specimen was carried out by Li (2017b) to investigate its seismic performance under high axial load. The experimental result of the CFDLT column specimen indicated that the CFDLT column has a potential of being used as a mega-column in super-tall buildings or mega-structures in the future.

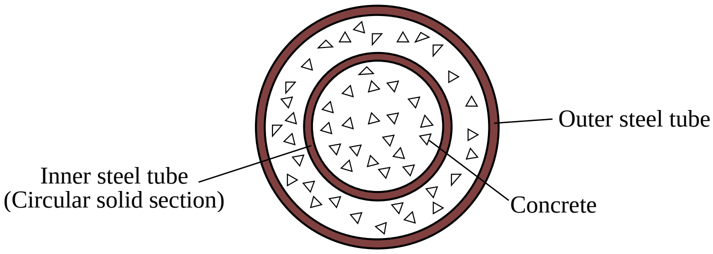

Figure 1. Cross-Section of concrete-filled double-layer steel tubular column (CFDLT column)

1.4 Multi-Cell CFT Column with Double-Layer Circular Steel Tubes

With increase of the structural height of super-tall building, the CFDLT column shown in Figure 1 might not meet the requirement of structural design. In order to satisfied structural demand, multi-cell CFT column with double-layer steel tubes can be selected. Figure 2 shows two examples of steel skeleton section of multi-cell CFT columns with double-layer circular steel tubes proposed in this study, which are developed from the CFDLT column through installing the required separating steel plates and required longitudinal stiffeners.

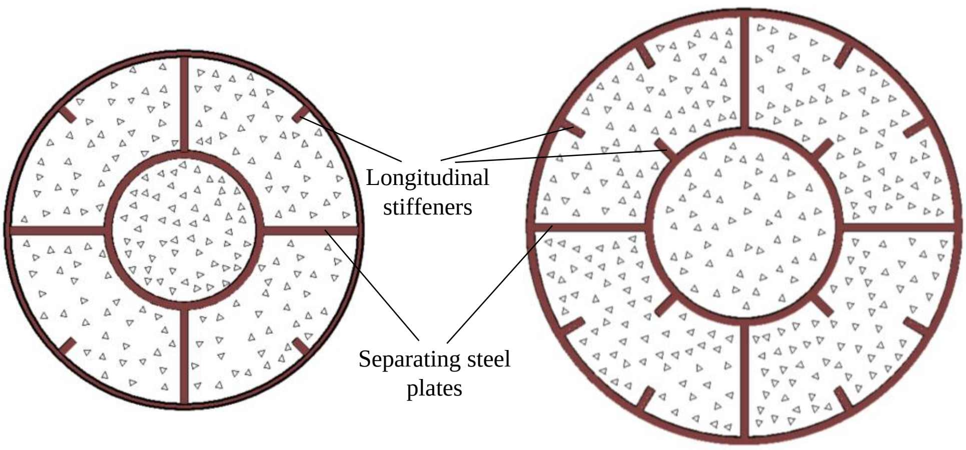

Figure 2. Multi-Cell CFT columns with double-layer circular steel tubes

1.5 Previous Numerical Study on CFDLT Column

Numerical study on the CFDLT column specimen was carried out by Li (2017c) using the finite-element analysis platform of OpenSees (Mazzoni et al. 2007). It was clarified that a simple combined constitutive model of concrete and steel tube can relatively accurately and safely evaluate the skeleton curve of the experimental lateral force-drift ratio relationship for the CFDLT column specimen even though the buckling behavior of steel tubes and compressive strength degradation of concrete are not considered. This simple combined constitutive model will shortly be introduced in Section 2.1 and Section 2.2.

1.6 Purpose of This Study

The purpose of this study is to investigate the contributions of the separating steel plates to the seismic performance of the multi-cell CFT column with double-layer circular steel tubes through numerical analyses.

2. SUMMARY OF SIMPLE COMBINED CONSTITUTIVE MODEL OF CONCRETE AND STEEL TUBE USED IN PREVIOUS NUMERICAL STUDY ON CFDLT COLUMN

2.1 Simple Constitutive Model of Concrete for CFDLT Column

The simple constitutive model of concrete for the CFDLT column proposed in previous work of Li (2017c) is shown in Figure 3. The σ_B is the concrete compressive strength (compression is negative) which is assigned a value as compressive strength of concrete cylinder. The ε_c is concrete strain once the compressive stress reaches the compressive strength (compression is negative), and the ε_c is defined as ε_c' which is the strain at compressive strength based on uniaxial compression test of the CFDLT column with the same cross-section and a height-diameter ratio equal to 3.0. In tension, the simple constitutive model of concrete was considered as Zero Tensile Strength model (no tensile strength).

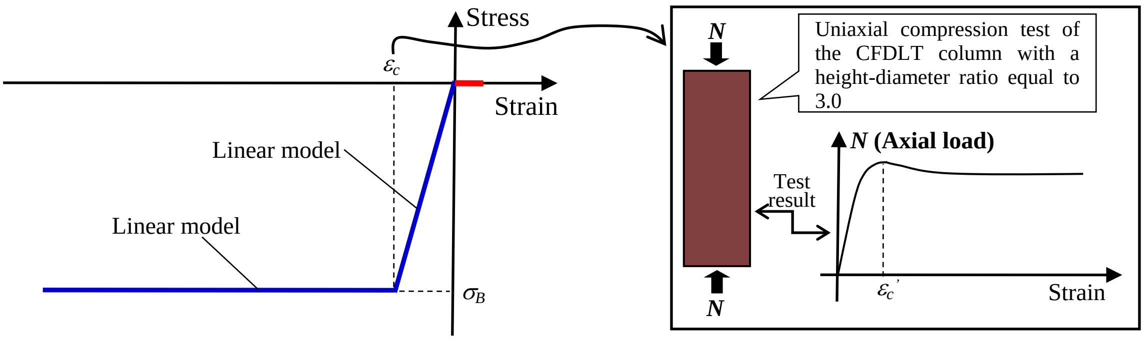

Figure 3. Concrete compressive pre-peak and post-peak response

2.2 Simple Constitutive Model of Steel Tubes for CFDLT Column

The constitutive model of the steel tubes for the CFDLT column proposed in previous work of Li (2017c) is shown in Figure 4. In this simple model with bilinear skeleton curve, strain-hardening ratio (ratio between post-yield tangent and initial elastic tangent), *b*, is defined as follows:

$$b = \frac{f_u' - f_y}{(\varepsilon_u' - \varepsilon_y) \cdot E_0} \tag{1}$$

where, f_y is the yield strength, ε_y is the yield strain, E_0 is the initial elastic tangent, and f_u' and ε_u' are the stress and the strain corresponding to the initial point of ultimate-strength plateaus, respectively.

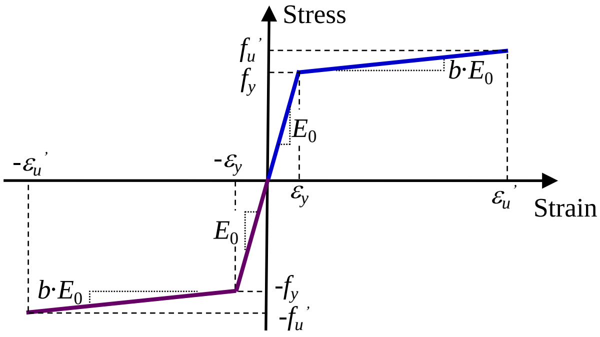

Figure 4. Constitutive law of steel tube

2.3 Summary of CFDLT Column Specimen in Previous Study

15-CFDLT is a concrete-filled double-layer steel tubular column specimen with circular solid section, which was the CFDLT column specimen in previous study of Li (2017b). The details of this specimen are illustrated in Figure 5. In column region of 15-CFDLT, diameter of cross-section is 190.7 mm, clear height is 800 mm, and shear span to depth ratio is about 2.1. The column has two concentric circular steel tubes. Outer steel tube and inner steel tube of 15-CFDLT are ϕ190.7 x 6 (outer diameter of 190.7 mm and thickness of 6 mm) and ϕ89.1 x 3.2, respectively. Axial force ratio of the column is 0.5. The steel ratio of column is 15.2%.

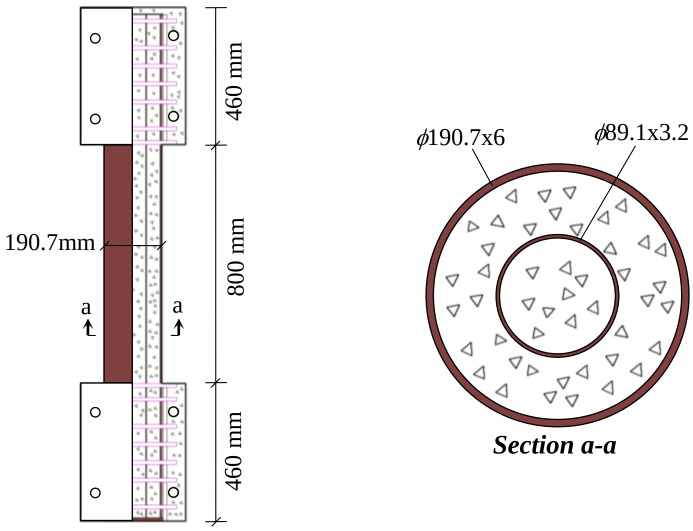

Figure 5. Details of 15-CFDLT

2.4 Comparison of Experimental Result and Numerical Result

The comparison of skeleton curve of experimental lateral force-drift ratio relationship in first quadrant and numerical lateral force-drift ratio response for 15-CFDLT is shown in Figure 6. In Figure 6, Q and R represent the lateral force and the drift ratio, respectively.

Figure 6 shows that the simple combined constitutive model of concrete and steel tube can relatively accurately and safely evaluate the skeleton curve of the experimental lateral force-drift ratio relationship for the column specimen 15-CFDLT.

Further details of the column specimen 15-CFDLT, experimental results of 15-CFDLT and experimental setup for 15-CFDLT can be investigated in the previous work of Li (2017b); further details of numerical modelling of 15-CFDLT can be investigated in reference of Li (2017c).

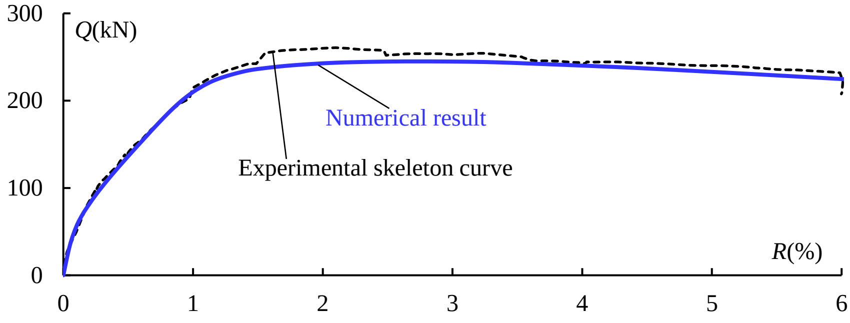

Figure 6. Comparison of experimental result and numerical result (15-CFDLT)

3. NUMERICAL STUDIES ON MULTI-CELL CFT COLUMNS WITH DOUBLE-LAYER CIRCULAR STEEL TUBES

The purpose of this study is to investigate the contributions of the separating steel plates to the seismic performance of the multi-cell CFT column with double-layer circular steel tubes. For investigation of the contributions as mentioned above, experimental tests can be the most reliable source. However, it is too costly and difficult to test actual multi-cell CFT column specimens. Instead, numerical analyses are selected to capture these contributions in this study. This chapter describes nonlinear numerical studies on simple multi-cell CFT (double-layer circular steel tubes) column specimens without longitudinal stiffeners based on OpenSees.

3.1 Column Specimens for Numerical Studies

A CFDLT column specimen and two simple multi-cell CFT column specimens are planned to investigate in this study through numerical analyses. The details of these three specimens are illustrated in Figure 7. The analysis parameters of them are summarized in Table 1. The mechanical

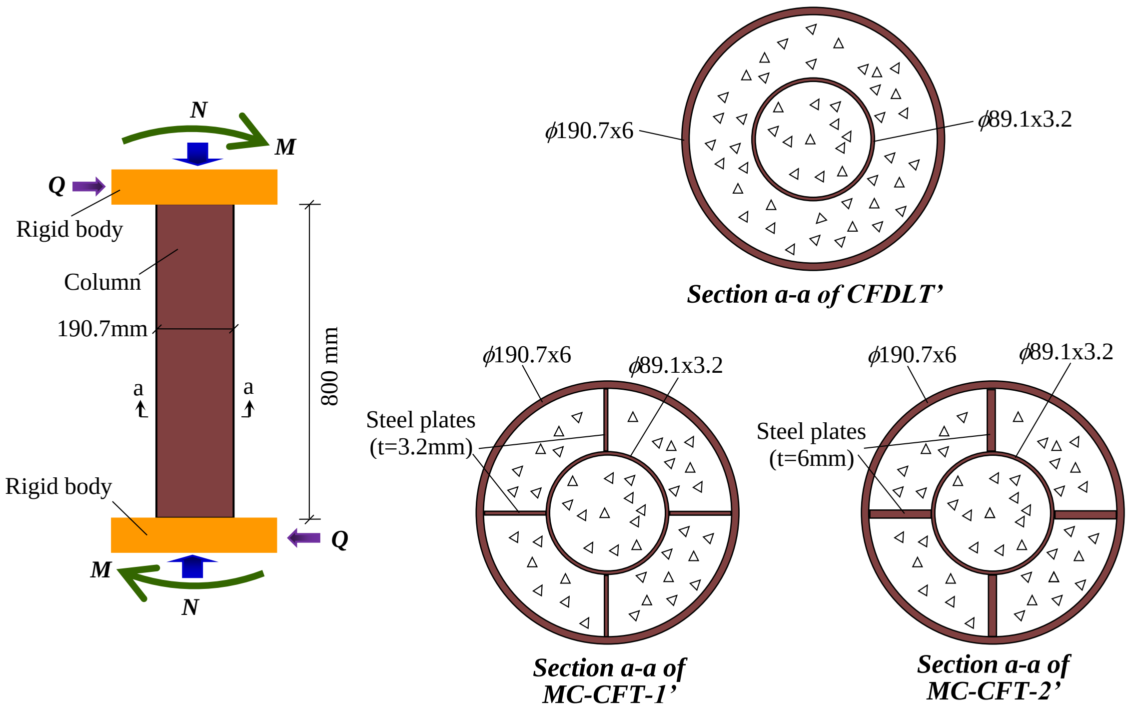

Figure 7. Details of column specimens for numerical studies

properties of steel tubes, separating steel plates and concrete used in these specimens are listed in Table 2.

CFDLT' is a conventional concrete-filled double-layer steel tubular column specimen. MC-CFT-1' and MC-CFT-2' are simple multi-cell CFT column specimens which are transformed from CFDLT' through installing four separating steel plates distributed uniformly between the outer steel tube and inner steel tube. Each specimen has two concentric circular steel tubes. In column region of every specimen, diameter of cross-section is 190.7 mm, clear height is 800 mm, and shear span to depth ratio is about 2.1. Outer steel tube and inner steel tube for each specimen are selected as ϕ190.7 x 6 and ϕ89.1 x 3.2, respectively. The shape of column region and sizes of outer steel tube and inner steel tube of each specimen are determined based on the specimen 15-CFDLT which has been introduced in Section 2.3. Thicknesses of the separating steel plates of MC-CFT-1' and MC-CFT-2' are chosen as 3.2 mm and 6 mm, respectively according to the thicknesses of their inner steel tubes and outer steel tubes.

All the steel tubes and separating steel plates used in the planned column specimens are considered to have the same material, and their mechanical properties are selected as those of the outer steel tube of 15-CFDLT. In addition, the mechanical properties of concrete of the planned column specimens are chosen to be the same with those of the concrete of 15-CFDLT.

CFDLT', MC-CFT-1' and MC-CFT-2' are considered to be subjected to antisymmetric bending moment and shear force under constant axial load. Axial force ratio of column region of CFDLT' is set at 0.5 which is the same ratio with that of 15-CFDLT. However, the axial loads on column regions of MC-CFT-1' and MC-CFT-2' are considered as the same load with that of CFDLT'.

Table 1. Analysis parameters of column specimens

Specimens	***N* or η_0**	**Outer tube**	**Inner tube**	**Separating plate**
CFDLT'	$\eta_0 = A_{so}\cdot f_{yo} + A_{si}\cdot f_{yi} + A_c\cdot \sigma_B{}' = 0.5$	ϕ190.7×6	ϕ89.1×3.2	———
MC-CFT-1'	Same *N* with CFDLT'	ϕ190.7×6	ϕ89.1×3.2	t=3.2mm
MC-CFT-2'	Same *N* with CFDLT'	ϕ190.7×6	ϕ89.1×3.2	t=6mm

Note: N = axial load on column, η_0 = axial force ratio of CFDLT', A_{so} = area of outer steel tube of CFDLT', A_{si} = area of inner steel tube of CFDLT', f_{yo} = yield strength of outer steel tube of CFDLT', f_{yi} = yield strength of inner steel tube of CFDLT', A_c = area of concrete in cross-section of CFDLT', $\sigma_B{}'$ = compressive strength of concrete cylinder of CFDLT'

Table 2. Mechanical properties of materials of column specimens for numerical studies

a) Steel

Categories	f_y	ε_y	E_0	σ_u	**%*EL***
ϕ190.7×6	389 MPa	0.174%	223 GPa	457 MPa	41.1%
ϕ89.1×3.2	389 MPa	0.174%	223 GPa	457 MPa	41.1%
PL-3.2	389 MPa	0.174%	223 GPa	457 MPa	41.1%
PL-6	389 MPa	0.174%	223 GPa	457 MPa	41.1%

Note: f_y = yield strength of steel, ε_y = yield strain of steel, E_0 = initial elastic tangent of steel, σ_u = ultimate strength of steel, %*EL* = percentage elongation of steel

b) Concrete

σ_B	ε_c
-59.4 MPa	-0.01

Note: σ_B = concrete compressive strength (compression is negative), ε_c = concrete strain once the compressive stress reaches the compressive strength (compression is negative)

3.2 Numerical Modelling with OpenSees

Figure 8 illustrates the numerical models of CFDLT', MC-CFT-1' and MC-CFT-2' in OpenSees. In each specimen, the column region is modelled with two element nodes and a two-dimensional nonlinear beam-column element with fiber sections located at the integration points. Every nonlinear beam-column element consists of eight integration points. Every fiber in each fiber section is under uniaxial state of stress. Each element node has three degrees-of-freedom. Element node 1 is fully fixed, and element node 2 is constrained on rotation only according to the boundary conditions.

In this study, the concrete is simulated with the Hysteretic Material in which the envelope of the compressive stress-strain response is defined using the simple constitutive model of concrete shown in Figure 3. The concrete strain once the compressive stress reaches the compressive strength, ε_c, is assigned a value of -0.01 according to the previous work of Li (2017c). In tension, the model of concrete is also considered as Zero Tensile Strength model which is the same with the simple constitutive model of concrete shown in Figure 3.

The outer steel tubes and inner steel tubes are simulated with Steel01 Material in which the envelope of the compressive stress-strain response and tensile stress-strain response are defined using the simple constitutive model shown in Figure 4. The monotonic compressive and tensile behavior of separating steel plates is also considered as the same behavior with the model shown in Figure 4. In this study, strain-hardening ratio, *b*, is assigned a value of 0.005 based on the previous work of Li (2017c).

For each column specimen, *P*-Delta coordinate transformation is adopted to perform a linear geometric transformation of stiffness and resisting force from the basic system to the global coordinate system, considering second-order *P*-Delta effects; Energy Increment Test is selected to specify a tolerance on the inner product of the unbalanced load and displacement increments at the current iteration; the modified Newton-Raphson algorithm is used to solve the nonlinear residual equation; an imposed lateral displacement, δ, is applied to element node 2 which is a control node (see Figure 8).

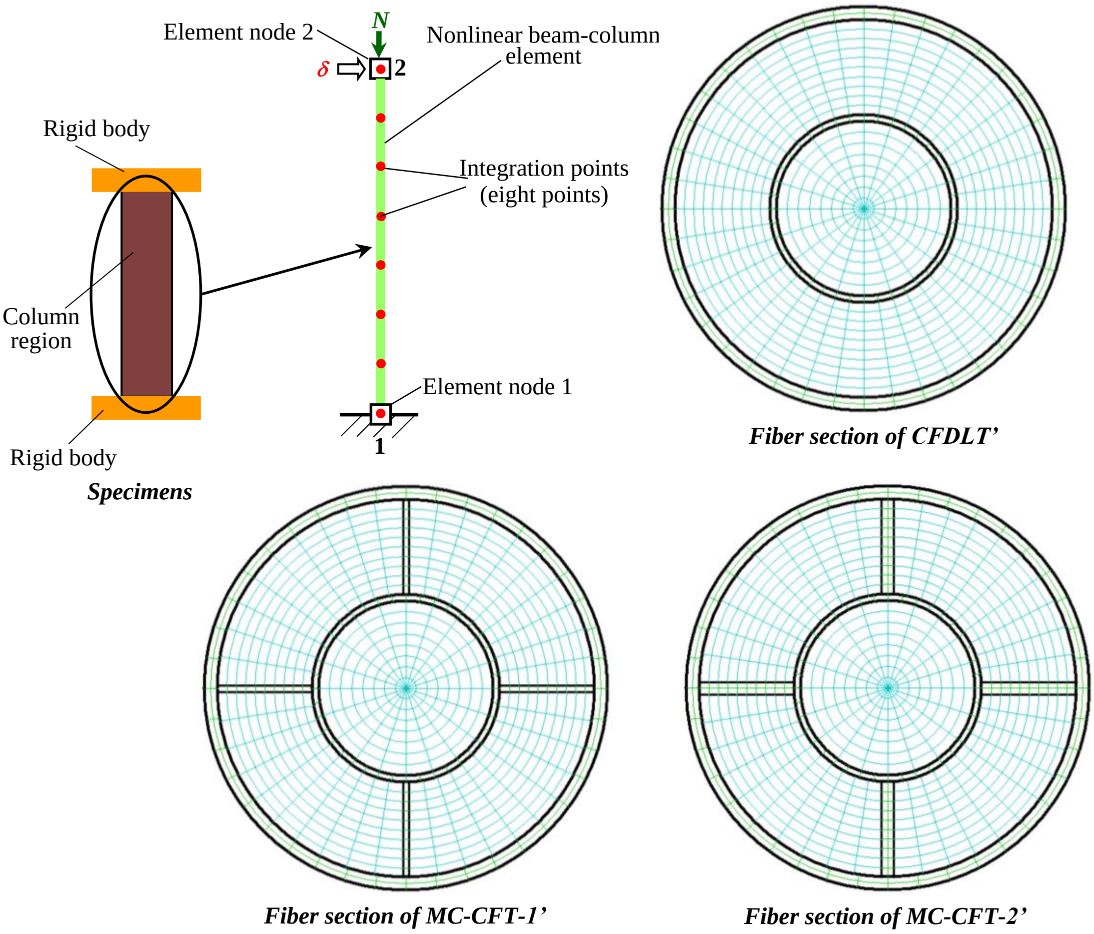

Figure 8. OpenSees models of column specimens

3.3 Numerical Results Based on OpenSees

The static pushover analyses are carried out based on the numerical models as mentioned in Section 3.2. The comparison of numerical lateral force-drift ratio response before drift ratio of 3.0% is shown in Figure 9.

Numerical flexural stiffness of MC-CFT-2' is higher than those of MC-CFT-1' and CFDLT'. Numerical lateral capacities of MC-CFT-2' and MC-CFT-1' are about 1.23 times and 1.13 times larger than that of CFDLT', respectively. The numerical results present the seismic performance of MC-CFT-2' is better than that of MC-CFT-1' because MC-CFT-2' has the thicker separating steel plates. CFDLT' shows the worst seismic performance because CFDLT' has no separating steel plate. It is proven that the separating steel plate can improve the flexural stiffness and increase the lateral capacity.

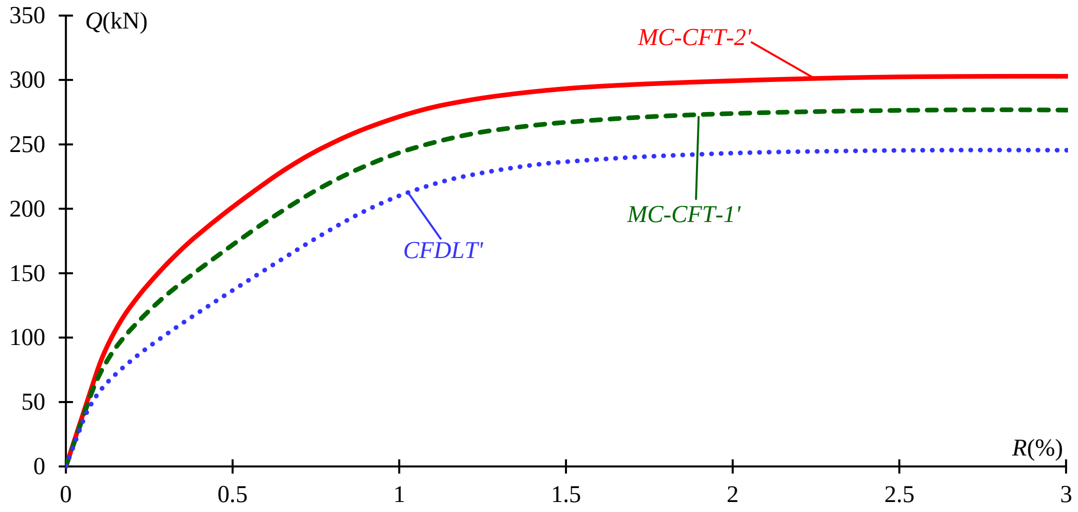

Figure 9. Comparison of numerical lateral force-drift ratio response

4. CONCLUSIONS

The following conclusions can be drawn from the above studies:

(1) Multi-cell CFT columns with double-layer circular steel tubes, separating steel plates and longitudinal stiffeners are proposed to meet the requirement of the structural design for the super-tall buildings in the future.

(2) Numerical lateral capacities of MC-CFT-2' and MC-CFT-1' are about 1.23 times and 1.13 times larger than that of CFDLT', respectively.

(3) The separating steel plate in the multi-cell CFT column can improve the flexural stiffness and increase the lateral capacity.

5. REFERENCES

Ding J, Chao S, Zhao X, Wu H (2011). Critical Issues of Structural Analysis for the Shanghai Center Project. *Journal of Building Structures*, 31(6): 122-131 (in Chinese).

Liu P, Yin C, Kevin L, Liu G, Huang X, Goman H, Alexis L (2012). Structural System Design and Study of Tianjin Goldin 117 Mega Tower. *Journal of Building Structures*, 42(3): 1-9 (in Chinese).

Liu P, Yin C, Cheng Y, Zhu Y, Liu Y, Wu H, Li X, Yang M, Liu H, Li Z (2014). Structural Design and Research of Beijing CBD Core Area Z15 Plot China Zun Tower. *Building Structure*, 44(24): 1-8 (in Chinese).

Mukai A et al. (1995-1998). U.S.-Japan Cooperative Structural Research Project on Composite and Hybrid Structures (CFT 1-CFT 35). *Summaries of Technical Papers of Annual Meeting (Architectural Institute of Japan)* (in Japanese).

Kawano A, Matsui C, Nakajima T, Takagi J (1996). Experimental Study on Buckling Behavior and Dissipated Energy of Concrete-Filled Tubular Members under Cyclic Axial Loading. *Journal of Structural and Construction Engineering*, No. 482: 131-140 (in Japanese).

Fujimoto T, Mukai A, Nishiyama I, Inai E, Kai M, Tanaka Y, Tokinoya H, Noguchi T, Baba T, Fukumoto N, Murata Y, Sakino K, Morino S (1997). Axial Compression Behavior of Concrete Filled Steel Tubular Stub Columns Using High Strength Materials. *Journal of Structural and Construction Engineering*, No. 498: 161-168 (in Japanese).

Tsuda K, Matsui C (1998). Inelastic Behavior of Circular Steel Tubular Beam-Columns under Constant Vertical and Alternating Horizontal Loads. *Journal of Structural and Construction Engineering*, No. 505: 131-138 (in Japanese).

Yamamoto T, Kawaguchi J, Morino S (2002). Experimental Study of the Size Effect on the Behavior of Concrete Filled Circular Steel Tube Columns under Axial Compression. *Journal of Structural and Construction Engineering*, No. 561: 237-244 (in Japanese).

Gould NC, Harmon TG (2002). Confined Concrete Columns Subjected to Axial Load, Cyclic Shear, and Cyclic Flexure - Part II: Experimental program. *ACI Structural Journal*, 99(1): 42-50.

Saisho M, Nakayama T, Gao S (2003). Local Buckling of Concrete Filled Circular Steel Tube Column. *Journal of Structural and Construction Engineering*, No. 567: 189-196 (in Japanese).

Georgios G, Dennis L (2004). Axial Capacity of Circular Concrete-Filled Tube Columns. *Journal of Constructional Steel Research*, 60(7): 1049-1068.

Li W (2017a). Seismic Performance of Concrete-Filled Double-Layer Steel Tubular Column under High Axial Load, *Proceedings of 39th International Association for Bridge and Structural Engineering Symposium-Engineering the Future*, 21-23 September, Vancouver, Canada, pp 1281-1288.

Li W (2017b). Study on Seismic Performance of Concrete-Filled Double-Layer Steel Tubular Column Subjected to High Axial Load. *Proceedings of the Japan Concrete Institute*, 39(2): 139-144 (in Japanese).

Li W (2017c). Numerical Study on Concrete-Filled Double-Layer Steel Tubular Column under High Axial Load, *6th Structural Engineers World Congress*, 14-17 November, Cancun, Mexico.

Mazzoni S, McKenna F, Scott M H, Fenves GL, et al. (2007). OpenSees Command Language Manual, The Regents of the University of California.